

# Gain Scheduled Active Power Control for Wind Turbines

Shu Wang\* and Peter Seiler†

*Department of Aerospace Engineering & Mechanics  
University of Minnesota, Minneapolis, MN, 55455, USA*

Traditional wind turbine control algorithms attempt to maximize power capture at low speeds and maintain rated power at high wind speeds. Active power control refers to a mode of operation where the turbine tracks a desired power reference command. Active power control enables wind farms to perform frequency regulation and to provide ancillary services in the energy markets. This paper presents a multiple input, multiple output strategy for active power control. An  $H_\infty$  controller is designed at several operating points to coordinate the blade pitch angle and generator torque. The objective is to track a given power reference command while also minimizing the structural loads. The controller is gain-scheduled based on the wind speed and the power output in order to compensate for the nonlinear turbine dynamics. This allows the turbine to be operated smoothly anywhere within the power / wind speed envelope. The performance of this gain-scheduled design is evaluated using high fidelity simulations.

## Nomenclature

$\rho$	Air density, $kg/m^2$
$v$	Wind speed, $m/s$
$A_r$	Rotor area, $m^2$
$\beta$	Blade pitch angle, $deg$
$\tau_g$	Generator torque, $N \cdot m$
$\lambda$	Tip speed ratio (TSR), unitless
$\omega$	Rotor speed, $rad/s$
$R$	Radius of rotor area, $m$
$P$	Generator power, $W$
$C_p$	Power coefficient, unitless
$N$	Gearbox ratio, unitless
$APC$	Active power control
$AGC$	Automatic generation control

## I. Introduction

As a promising renewable energy, wind power is increasing fast in energy markets all over the world. Though it only accounts for 3% of the electricity produced globally in 2011, the penetration of wind energy is very high in some European countries.<sup>1</sup> In the United States, the amount of wind energy is expected to increase to about 30% by 2020 to 2030.<sup>2</sup> The power output of wind turbines is variable due to time-varying wind speeds and this may cause unreliable operation of the power grid. This is not a significant issue when wind power is only a small portion of the total electricity generated on the grid. However, to integrate higher levels of variable wind power into the grid it is important for wind turbines to provide active power control (APC).<sup>3</sup> APC can be used for the turbine to respond to fluctuations in grid frequency, termed primary

---

\*Graduate Student, wang2927@umn.edu

†Assistant Professor, seiler017@umn.edu

response, and to the power curtailment command from transmission system operator, termed secondary response or automatic generation control (AGC).<sup>4</sup>

Traditional wind turbine control systems<sup>5</sup> do not provide active power control. The power electronics used in variable speed wind turbines decouple the mechanical/inertial turbine dynamics from the power grid. Thus a wind turbine with a traditional control law does not have the inertial response to a grid frequency event like a conventional coal power generator.<sup>6</sup> As a result the wind turbine does not participate in the primary response. Moreover, the power output from the turbine fluctuates with variations in wind speed. As a result, new control strategies are being considered to enable wind turbines to track power commands and possibly provide ancillary services.<sup>7-12</sup> Some of these designs provide primary response by using inertia response emulation.<sup>7,8</sup> Another approach is to operate the wind turbine above the optimal tip speed ratio thus reserving kinetic energy.<sup>9,10</sup> This approach enables the wind turbine to track the power commands and hence this can be used to realize AGC. The use of blade pitch control with or without combined generator torque control has also been explored.<sup>11,12</sup>

This paper proposes a gain-scheduled  $H_\infty$  controller to provide APC. The architecture is a 2-input, 2-output controller where collective blade pitch and generator torque are coordinated in order to track power and rotor speed reference commands. The controller is scheduled on the wind speed and power output. This enables the gain-scheduled controller to have a uniform structure and operate smoothly anywhere within the power/wind speed envelope of the turbine. Compared with a standard LPV controller<sup>13,14</sup> which is solved from linear matrix inequalities, the gain scheduling in this paper is realized by linear interpolation of the LTI controllers designed at grid points in the envelope. This simplifies the design process and allows for smooth transitions of the closed-loop system between low and high wind speed operation. The remainder of the paper is organized as follows. Section II briefly reviews traditional turbine control and describes the proposed gain-scheduling approach for APC. Section III gives the detailed design process for the gain scheduled  $H_\infty$  controller. Simulation results are presented and discussed in Section IV. Finally, conclusions and future work are summarized in Section V.

## II. Control Strategy Development for APC

The proposed strategy for active power control of an individual turbine is developed in this section. Section II.A briefly reviews the traditional operation and control for a utility-scale wind turbine. The new active power control strategy is described in Section II.B.

### A. Traditional Wind Turbine Control

The captured power is given by  $P_c = \frac{1}{2}\rho A_r v^3 C_p(\beta, \lambda)$  where  $\rho$  is the air density [ $kg/m^3$ ],  $A_r$  is the swept area of the rotor blades perpendicular to the wind flow [ $m^2$ ], and  $v$  is the wind speed [ $m/s$ ].<sup>5,15</sup> The non-dimensional power coefficient  $C_p$  is the fraction of the available wind power captured by the turbine. The power coefficient is a function of the (collective) blade pitch angle  $\beta$  [ $deg$ ] and the tip speed ratio  $\lambda$  [*unitless*]. The tip speed ratio is defined as the ratio  $\lambda := \frac{R\omega}{v}$  where  $\omega$  is the rotor speed [ $rad/s$ ] (low speed side of the drive train) and  $R$  is the radius of the rotor area [ $m$ ]. In words,  $\lambda$  is defined as the blade tip tangential velocity divided by the wind speed. Figure 1 shows a contour plot of the power coefficient  $C_p$  as a function of the blade pitch  $\beta$  and tip speed ratio  $\lambda$ . The contours are shown for the WindPACT 1.5 MW turbine model provided with the NREL FAST turbine simulation package.<sup>16</sup> The main control inputs to operate the turbine are the blade pitch angle  $\beta$  and generator torque  $\tau_g$  [ $N \cdot m$ ].

The trade-off between power capture and load reduction is typically achieved using a mode-dependent controller with objectives that depend on the wind speed.<sup>5,17,18</sup> There are essentially four operating regions as shown in the power versus wind speed curve in Figure 2. Below the cut-in speed (Region 1), there is insufficient wind and the turbine is kept in a parked, non-rotating state. Above the cut-out speed (Region 4), the turbine is shut down to prevent structural damage.

Between the cut-in and rated wind speeds (Region 2), the objective is to maximize the captured power. As shown in Figure 1, the power coefficient attains its optimal value of  $C_{p*} = .5075$  when  $\lambda_* = 7.2$  and  $\beta_* = 1.4 deg$ . Thus power capture is maximized by holding blade pitch constant at  $\beta_*$  and commanding the generator torque such that the turbine operates at  $\lambda_*$ . It can be shown that the standard control law<sup>18,19</sup>

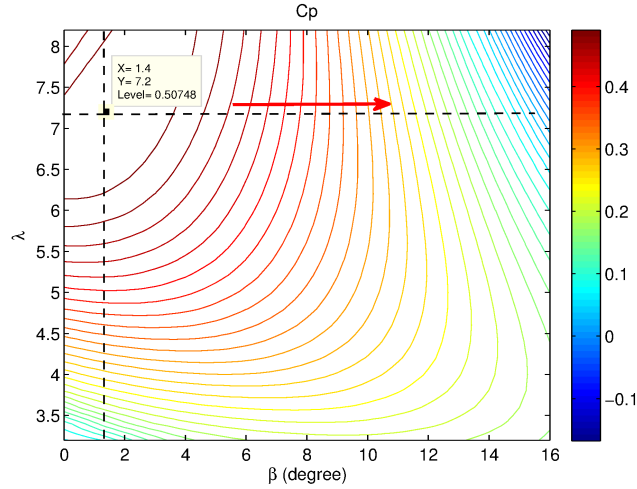


Figure 1. Power coefficient contours for WindPACT 1.5MW Model.

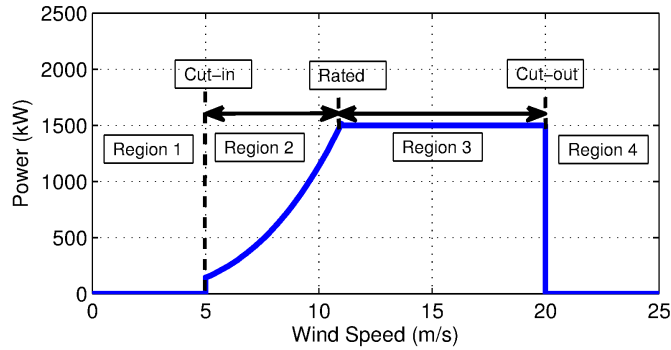


Figure 2. Turbine operating regions.

$\tau_g = K_g \omega^2$  achieves this goal in steady winds if the gain is chosen as

$$K_g = \frac{C_{p*} \rho A R^3}{2 \lambda_*^3 N} \quad (1)$$

where  $N$  [unitless] is the gearbox ratio.

Between the rated and cut-out wind speeds (Region 3), the objective is to maintain the rated power while minimizing the structural loads on the turbine. In Region 3, the generator torque can be held constant and the blade pitch angles are actively controlled to maintain rotor speed at its rated value. Classical PI or PID controllers<sup>18,19</sup> are widely used for the blade pitch control. Many methods have also been developed to improve the load reduction performance in this region, e.g. individual pitch control,<sup>20,21</sup> LIDAR feed-forward,<sup>22,23</sup> and advanced modern control methods.<sup>24-26</sup> Blending is used as the wind speed approaches the rated wind speed to ensure smooth transition between the Region 2 and Region 3 control objectives. The transition between Regions 2 and 3 is sometimes referred to as Region 2.5. Region 2.5 is introduced because the rated rotor speed is usually reached before the Region 2 control law reaches the rated torque. A linear torque vs. rotor speed relation is typically used to ramp from the standard  $\tau_g = K_g \omega^2$  to the rated torque.<sup>5</sup>

## B. Architecture for APC

The traditional turbine control system reviewed in Section II.A does not provide active power control. This section describes the proposed approach to provide the capability to track power reference commands. It is

important to note that the wind conditions limit the power that can be generated (in steady-state) by the turbine. Specifically, the turbine must operate within the power vs. wind speed envelope shown in Figure 2. Thus active power control is constrained to power reference commands that are within this envelope. Methods to reserve power and operate within this envelope include de-rating, relative spinning reserve, and absolute spinning reserve.<sup>10,12,27</sup> Each of these methods corresponds to operation along a specific power vs. wind speed curve that lies within the available power envelope.

Our proposed approach is to use gain scheduling to operate anywhere within the power envelope. This would enable de-rating, relative spinning reserve, and absolute spinning reserve as special cases. The basic operational concept is shown in Figure 3. Trim points, denoted by red x's, are chosen at many points on a grid within the power curve. At each trim point, the turbine dynamics are linearized and a control law is designed using linear design techniques. Linear interpolation is used to calculate the controller gains for operation between trim points, i.e. the controller is gain scheduled based on trim power and wind condition. Details on this design and implementation are provided in the next section. The gain scheduling approach described here is less rigorous than modern linear parameter varying (LPV) techniques.<sup>28,29</sup> The LPV design techniques account for time variations in the scheduling variables. The gain scheduling proposed here should be sufficient for slow variations in the scheduling parameters although there are no formal performance guarantees. The benefit of gain-scheduling, as compared to more formal LPV techniques, is the ease of design and implementation.

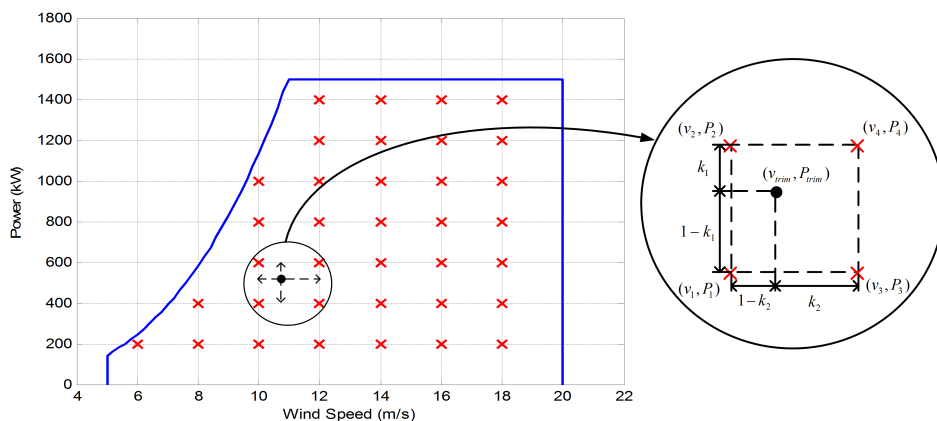


Figure 3. Operation envelope for gain scheduling.

The control design at a single trim point is now briefly described. To operate at one of the  $(v, P)$  trim conditions within the envelope, the turbine must reduce the power coefficient to a new value  $C_p < C_{p*}$  by changing the blade pitch angle and/or the tip speed ratio. As shown in Figure 1, there is a contour of possible values of  $(\lambda, \beta)$  that achieve any value of  $C_p < C_{p*}$ . For a given  $(v, P)$  trim condition, the controller can be designed to operate at any point on the new  $C_p$  contour. For example, in low wind speeds the controller proposed in<sup>10</sup> shifts from  $(\lambda_*, \beta_*)$  to a larger tip speed ratio  $\lambda > \lambda_*$  while holding blade pitch fixed at  $\beta_*$ . The benefit of this approach is that the turbine operates at a higher rotor speed and hence retains kinetic energy that can be extracted at a later point in time. To summarize, each  $(v, P)$  trim condition corresponds to a desired power coefficient. The selection of  $(\lambda, \beta)$  along the contour of this desired  $C_p$  enables a secondary performance objective to be achieved, e.g. stored kinetic energy, reduced structural loads, etc.

The controller proposed in this paper tracks the desired power as follows. In low wind speeds, the controller shifts from  $(\lambda_*, \beta_*)$  to the desired  $C_p$  by increasing to a larger blade pitch  $\beta > \beta_*$  while holding tip speed ratio fixed at  $\lambda_*$ . The red arrow in Figure 1 indicates the proposed shift to the desired  $C_p$  in low wind speeds. In constant wind conditions, this approach holds desired rotor speed constant (to maintain  $\lambda_*$ ) while blade pitch angle is increased to shed extra power according to the desired power command. The benefit is that the constant loads on the blade, tower, and gearbox should be reduced by this method of shedding power. However, this approach has the drawback that it will increase the pitch actuator usage. Another drawback of this approach is that less kinetic energy is retained in the rotor than if the turbine were to shift to a larger tip speed ratio.

The APC strategy proposed in this paper can be implemented as the control system structure shown in

Figure 4. A 2-input, 2-output control system is used to coordinate the blade pitch and generator torque. The main objective is to track the power reference command  $P_{cmd}$ . The rotor speed command  $\omega_{cmd}$  specifies the desired point on the power coefficient contour. In particular the rotor speed command is defined as follows:

$$\omega_{cmd} = \min \left\{ \frac{v_{trim} \lambda_*}{R}, w_{rated} \right\} \quad (2)$$

where  $w_{rated}$  is the rated rotor speed and  $v_{trim}$  is an estimate of the effective wind speed. As described above, this rotor speed command attempts to keep the  $\lambda$  at the optimal value  $\lambda_*$  at lower wind speeds. This will cause an increasing rotor speed demand as wind speed increases. At higher wind speeds, the rotor speed command saturates and attempts to maintain the rated rotor speed. It is assumed that an accurate and real time measurement of the wind speed is available. As shown in Figure 4, an estimate of the wind speed could be obtained from a LIDAR.<sup>30</sup> Alternatively, an estimate of the effective wind speed could be constructed.<sup>31</sup> In either case, the actual wind speed fluctuates and hence low-pass filtering, denoted LPF1 in the figure, is used to smooth out these fluctuations.

The use of gain-scheduling with this MIMO architecture allows for uniform performance of the turbine across all wind conditions. In other words, controllers of the same structure can be integrated using the technique of gain scheduling to meet the requirements in different wind conditions. The performance of the control system should be uniform and easy to design. The problem of transferring between regions of operations will also be a natural procedure in the design. However, it should be noted that this combined MIMO control structure is more complicated than the SISO loops used in traditional wind turbine control. This may limit the ease of transitioning the proposed method to industrial turbines. A variety of simpler control architectures for APC were proposed and compared by Jeong, et. al.<sup>12</sup>

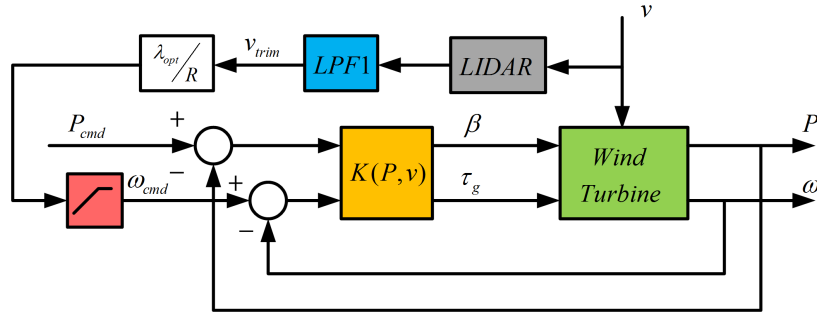


Figure 4. Proposed control strategy for APC.

### III. Gain Scheduled $H_\infty$ Control Synthesis

This section provides details on the gain-scheduled approach introduced in Section II. The controller is designed for the WindPACT 1.5 MW wind turbine whose model is contained in the FAST simulation package.<sup>16</sup> First, the one-state rotor dynamic model is linearized at an arbitrary trim condition. Next,  $H_\infty$  control design is described for one trim condition. Finally, details are provided for the gain-scheduling approach.

#### A. Linearized Model For Control Design

The FAST simulation package developed by NREL<sup>16</sup> is a nonlinear simulation package that is widely used for wind turbine control and analysis. This model includes up to 24 degrees of freedom, including different tower and blade bending modes. FAST models can be linearized at a steady wind speed to obtain a periodic, linear time-varying model. The multi-blade coordinate transformation can then be applied to obtain an approximate linear time-invariant model. The resulting linear time invariant models are suitable for advanced control design. However, to simplify the synthesis of the gain scheduled controller this paper uses the one-state rotor model (described below) for design. The nonlinear one-state rotor model captures the essential aerodynamics and rotor dynamics of a wind turbine.<sup>19</sup> This model does not contain structural dynamics but it simplifies the design and it is useful for understanding the effectiveness of the proposed

active power control strategy. Moreover, the one-state model is only used for design but the controller is evaluated using higher fidelity simulations within FAST.

The one-state rotor model is given by:

$$J\dot{\omega} = \tau_a - N\tau_g \quad (3)$$

where  $\tau_a$  and  $\tau_g$  [ $N \cdot m$ ] are the aerodynamic and generator torques on the drive train.  $J$  [ $kg \cdot m^2$ ] is the inertia of all rotating parts, including the blades, hub and drive train.  $\omega$  [ $rad/s$ ] is the rotor speed on the low speed side of the drive train. The aerodynamic torque can be expressed in terms of the captured power as

$$\tau_a = \frac{P_a}{\omega} = \frac{C_p \rho A v^3}{2\omega} \quad (4)$$

The generator power output is given by

$$P = EN\tau_g\omega \quad (5)$$

where  $E$  is the generator efficiency.

The model used here also includes the standard control law in Equation 1 as an inner loop of the turbine dynamics and part of the system to be controlled. This inner loop is helpful to maintain stability of the turbine. The analysis will be provided later. Moreover, retaining this inner loop feedback enables the potential to shift smoothly between APC and the traditional torque control. Therefore,  $\tau_g$  is given by:

$$\tau_g = \tau + K_g\omega^2 \quad (6)$$

where  $\tau$  [ $N \cdot m$ ] is the torque commanded by the outer loop for APC.

The model used for control design is obtained by linearizing this nonlinear system at a trim condition. Since the objective is to control the power output, a specific power  $P_0$  and wind speed  $v_0$  are selected for trim condition. The trim rotor speed  $\omega_0$  can then be calculated from  $v_0$  based on the rotor speed command in Equation 2. The trim generator torque is calculated from  $\tau_{g0} = \frac{P_0}{EN\omega_0}$ .  $C_{p0}$  is derived from the ratio of trim generator power  $P_0$  to the power available from the wind. Finally, the trim collective blade pitch  $\beta_0$  is found from the  $C_{p0}$  contour data. Table 1 shows a single trim condition used for linearizing the WindPACT model.

**Table 1. WindPACT Trim Condition**

Parameter	Value
$v_0$ (m/s)	8
$P_0$ (kW)	400
$\omega_0$ (RPM)	15.715
$\tau_{g0}$ ( $N \cdot m$ )	2909.3
$C_{p0}$	0.34896
$\beta_0$ (deg)	8.9289

Let  $\Delta$  be used to denote the deviation of a variable from its trim condition, e.g.  $\Delta\omega := \omega - \omega_0$  denotes the deviation of the rotor speed from the trim operating condition. The linearization of the nonlinear rotor model is given by a state space model of the form

$$\dot{x} = Ax + \begin{bmatrix} B_\beta & B_\tau \end{bmatrix} u + B_v \Delta v \quad (7)$$

$$y = \begin{bmatrix} EN(\tau_{g0} + 2K_g\omega_0^2) \\ 1 \end{bmatrix} x + \begin{bmatrix} 0 & EN\omega_0 \\ 0 & 0 \end{bmatrix} u + \begin{bmatrix} 0 \\ 0 \end{bmatrix} \Delta v \quad (8)$$

$x := \Delta\omega$  is the state,  $u := \begin{bmatrix} \Delta\beta \\ \Delta\tau \end{bmatrix}$  is the vector of control inputs, and  $y := \begin{bmatrix} \Delta P \\ \Delta\omega \end{bmatrix}$  is the vector of system

outputs. The state matrices are given by:

$$A = \left( -C_{p0} + \lambda_0 \frac{\partial C_p}{\partial \lambda} \right) \frac{\rho A_r v_0^3}{2J\omega_0^2} - \frac{C_{p*} \rho A_r R^3}{J\lambda_*^3} \omega_0 \quad (9)$$

$$B_\beta = \frac{\partial C_p}{\partial \beta} \frac{\rho A_r v_0^3}{2J\omega_0} \quad (10)$$

$$B_\tau = -\frac{N}{J} \quad (11)$$

$$B_v = \left( 3C_{p0} - \lambda_0 \frac{\partial C_p}{\partial \lambda} \right) \frac{\rho A_r v_0^2}{2J\omega_0} \quad (12)$$

For the trim condition in Table 1, the partials derivatives appearing in this linearization are  $\frac{\partial C_p}{\partial \lambda} = 0.0017$  and  $\frac{\partial C_p}{\partial \beta} = -2.1486$ . Some parameters of the system are listed here:  $A = -0.1104$ ,  $B_\beta = -0.4624$ ,  $B_\tau = -2.5816 \times 10^{-5}$  and  $B_v = 0.0278$ . The second term of the state matrix  $A$  is  $-\frac{C_{p*} \rho A_r R^3}{J\lambda_*^3} \omega_0$ . This term arises from the inner-loop standard law feedback and it is helpful to ensure the stability of the turbine dynamics.

## B. $H_\infty$ Synthesis at One Trim Condition

This section describes the APC design at a single operating condition using the linearized one-state model presented in the previous subsection. The proposed control architecture in Figure 4 uses collective blade pitch and generator torque in order to track power and rotor speed commands. In principle, the controller could be implemented using the decoupled system shown in Figure 5. In this diagram  $G(s)$  denotes the linearized one-state rotor dynamics and  $A_\beta(s)$  denotes the dynamics of the blade pitch actuator. The dynamics of the blade pitch actuator are modeled as a low pass filter  $A_\beta(s) = \frac{1}{s+1}$ . In this decoupled structure, the blade pitch is used to track power reference commands. The blade pitch actuation shifts the power coefficient based on the power tracking error and this causes a change in the aerodynamic torque  $\tau_a$ . The generator torque is used to track the rotor speed commands. The decoupled controllers in this architecture,  $K_\beta(s)$  and  $K_\tau(s)$ , could be simple classical controllers, e.g. PI controllers, designed to achieve the tracking objectives.

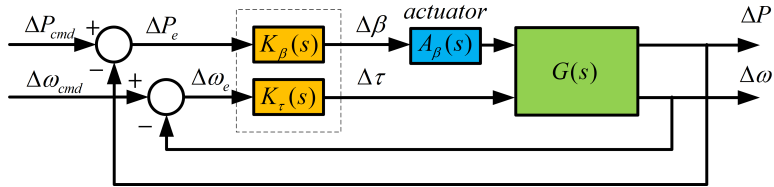


Figure 5. Decoupled Controller Architecture

This decoupled structure is simple and easy to understand. However, it complicates the control design because the turbine dynamics couple together the power and rotor speed. This dynamic coupling makes it difficult to properly tune the independent controllers  $K_\beta(s)$  and  $K_\tau(s)$ . Moreover, the gain scheduling design described in Section II.B requires controllers to be designed at many different trim points. Thus, manual tuning of the controllers in this decoupled architecture would be time consuming and it would be difficult to achieve uniform performance across the entire operational envelope.

For these reasons  $H_\infty$  synthesis<sup>32,33</sup> is applied in this paper to design coupled MIMO controllers. This methodology should enhance the performance by properly coordinating the two control inputs. Moreover, performance weights can be specified to enable tuning of the controller at many trim conditions. The augmented system for  $H_\infty$  synthesis is shown in Figure 6. Here, seven different weight functions are chosen to specify the performance requirements. The choice for each of these weights is described in detail below.

$W_1(s)$  and  $W_2(s)$  are two performance weights that specify the objectives for power and rotor speed tracking. These weights are chosen to limit the low frequency error with less emphasis on high frequency tracking. The bandwidth of the power tracking weight is selected to be  $0.08 \text{ rad/s}$ . This is a conservative bandwidth but it is sufficiently fast for many power tracking objectives, e.g. AGC. The low frequency gain is 5000 which corresponds to a desired steady-state error in power tracking of  $0.2 \text{ kW}$ . This enforces a very tight power tracking requirement in steady state. Finally, the performance weight on the power tracking

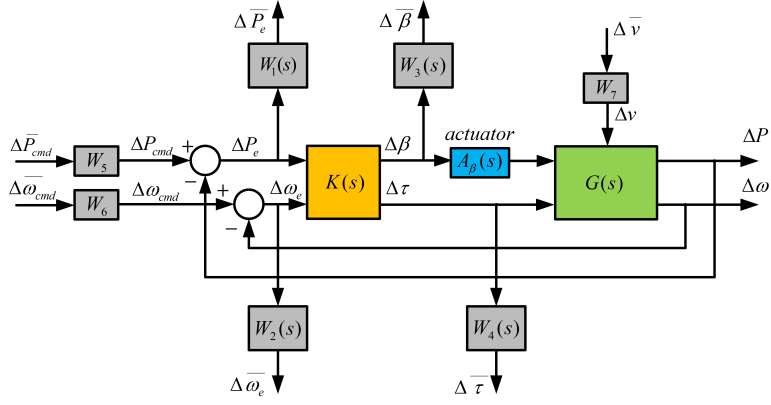


Figure 6. Augmented system for  $H_\infty$  synthesis.

error is given by:

$$W_1(s) = 5 \frac{100s + 21}{200s + 0.021} \quad (13)$$

The weight on rotor speed error  $W_2(s)$  is chosen similarly:

$$W_2(s) = 2.5 \frac{100s + 13}{200s + 0.013} \quad (14)$$

Next,  $W_3(s)$  and  $W_4(s)$  are two weights used to penalize the actuation of blade pitch angle and generator torque, respectively. Both weights are chosen as high pass filters to penalize high frequency control effort.  $W_3(s)$  is chosen to have a bandwidth of  $0.15 \text{ rad/s}$  and this weight is specified as:

$$W_3(s) = \frac{2.5}{\pi} \frac{1000s + 11}{s + 21} \quad (15)$$

The generator torque can be actuated sufficiently fast that its actuator dynamics can be neglected. However, the weight  $W_4(s)$  is still required to avoid aggressive generator torque commands and hence accommodate the use of the blade pitch actuator whose bandwidth is relatively narrow. This enables the proper coordinate of the two control inputs. The weight  $W_4(s)$  is chosen as:

$$W_4(s) = \frac{1}{2000} \frac{100s + 14}{s + 140} \quad (16)$$

Finally, the weights  $W_5 = 0.2$ ,  $W_6 = 0.4$  and  $W_7 = 1.4$  are used to scale the input power command, and rotor speed command, and wind disturbance to values corresponding to  $0.2 \text{ MW}$ ,  $0.4 \text{ rad/s}$  and  $1.4 \text{ m/s}$ , respectively. Once the weights have been selected, the synthesis of the  $H_\infty$  controller at any trim condition can easily be performed using standard commands in Matlab. The performance of each  $H_\infty$  control design around the design trim condition was evaluated using high fidelity simulations with FAST. Some of these results are provided in Section IV.A.

### C. Gain Scheduled Control Synthesis

The previous subsection introduced the  $H_\infty$  synthesis for APC at a specific trim condition. Due to the nonlinear turbine dynamics the performance of this single controller may only be acceptable for a relatively small range around the trim power and wind speed trim point. The technique of gain scheduling is used here to cover the entire working envelope. Compared with a standard LPV controller,<sup>13,14</sup> a gain-scheduled controller is relatively easy to design. In particular, the formal LPV methods require the solution of linear matrix inequalities that ensure guarantee performance. Gain scheduling, as used here, simply refers to linear interpolation of the  $H_\infty$  point designs and hence is less computationally intensive to design. However, this use of linear interpolation offers no performance guarantees.

Figure 3 shows the working envelope of the wind turbine. The design in Section III.B is based on a specific point in this envelope. For the preparation of the gain scheduling design, 36 trim points are chosen

uniformly in increments of  $200 \text{ kW}$  in power and  $2 \text{ m/s}$  in wind speed. These 36 trim points are denoted by  $x$ 's in Figure 3.  $H_\infty$  controllers are designed at each trim condition using the same weights given in Section III.B.

Gain scheduling is used to interpolate the point control designs and their corresponding trim conditions. The detailed gain-scheduled structure is shown in Figure 7. Wind speed and power output signals are low pass filtered and sent to the controller as trim conditions  $v_{trim}$  and  $P_{trim}$ . The wind speed signal is the same as that used to calculate the rotor speed reference command. The two low pass filters are chosen after some trial and error to have corner frequencies of  $0.1 \text{ rad/s}$  (LPF 1) and  $0.04 \text{ rad/s}$  (LPF 2).

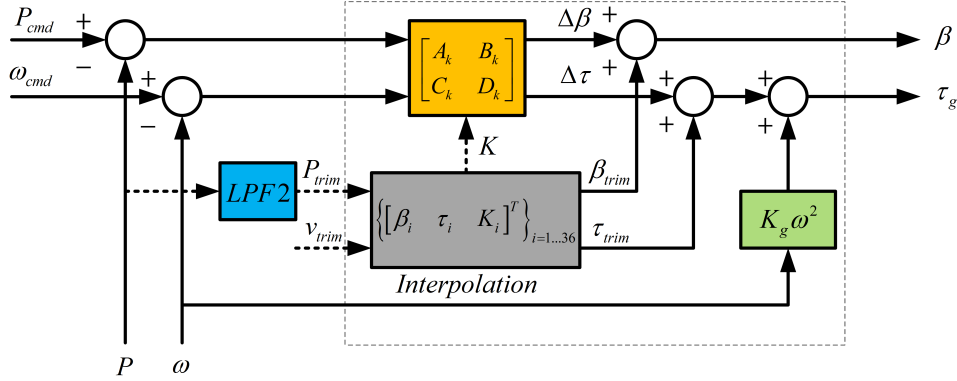


Figure 7. Structure of the gain scheduled controller.

The trim values of blade pitch angle  $\beta_{trim}$  and generator torque  $\tau_{trim}$  are calculated by linear interpolation. Specifically, the four nearest “grid” trim points  $\{v_i, P_i\}_{i=1}^4$  of the current  $(v_{trim}, P_{trim})$  are determined as shown in Figure 3. The fractional distance along each coordinate axis is computed as  $k_1 = \frac{P_2 - P_{trim}}{P_2 - P_1}$  and  $k_2 = \frac{v_3 - v_{trim}}{v_3 - P_1}$ . Finally, the trim blade pitch and generator torque is given by

$$\begin{bmatrix} \beta_{trim} \\ \tau_{trim} \end{bmatrix} = k_2 \left( k_1 \begin{bmatrix} \beta_1 \\ \tau_1 \end{bmatrix} + (1 - k_1) \begin{bmatrix} \beta_2 \\ \tau_2 \end{bmatrix} \right) + (1 - k_2) \left( k_1 \begin{bmatrix} \beta_3 \\ \tau_3 \end{bmatrix} + (1 - k_1) \begin{bmatrix} \beta_4 \\ \tau_4 \end{bmatrix} \right) \quad (17)$$

Some trim conditions near the boundary of the operating area have less than four neighboring “grid” trim points. For conditions with only two neighbors, the interpolation is along a single dimension. For conditions with only three neighbors, the fourth missing interpolant is filled using the grid condition that occurs at the same trim wind speed. The state-space matrices for the controller,  $\begin{bmatrix} A_k & B_k \\ C_k & D_k \end{bmatrix}$  are interpolated in a similar fashion as that given in Equation 17. As shown in Figure 7, the trim inputs  $\beta_{trim}$  and  $\tau_{trim}$  are added to the control inputs  $\Delta\beta$  and  $\Delta\tau$  generated by the scheduled controller  $K$ . The standard torque feedback is used as an additional inner loop feedback for stabilizing the system as described in Section III.A.

## IV. Simulation Results

### A. Simulation for A Single LTI Controller

The first group of simulations were performed on both the linearized one state model of Wind PACT 1.5 MW wind turbine and the corresponding nonlinear model in FAST. The structural modes in the FAST model include the first flap-wise blade mode for each blade and the first fore-aft tower bending mode. Including the rotor position, the model has five degrees of freedom. This is a general setting for all the simulations in FAST. Both simulations only use an  $H_\infty$  controller designed at one trim condition as described in Section III.B. The controller was designed at the steady wind speed of  $8 \text{ m/s}$  and trim power of  $400 \text{ kW}$ . The maximum captured power at this wind speed is  $581 \text{ kW}$ .

Two simulation results are shown in Figure 8. The left subplots show the results for a power command signal that steps from  $400 \text{ kW}$  to  $450 \text{ kW}$  at  $t = 50 \text{ s}$  and then back to  $400 \text{ kW}$  at  $t = 150 \text{ s}$ . The wind

speed was held constant at the trim condition. The left subplots show, from top to bottom, the rotor speed response, power output, blade pitch angle, and generator torque. Results are shown for both the linear (dashed) and nonlinear (solid) simulations. These simulation results show good agreement between the nonlinear FAST and linear simulations. The generator power output reached the new level by 90% in less than 10 s without overshoot. The rotor speed fluctuation was also well regulated.

The right subplots in Figure 8 show the simulation results for a power step command from 400 kW to 550 kW and then back. The wind speed was again held constant at the trim condition. The linear and nonlinear simulations show similar power tracking performance. However, the nonlinear simulations show some discrepancies in the rotor speed and blade pitch angle responses. These discrepancies are due to the nonlinear turbine dynamics which become more significant for larger deviations from the trim operating condition. In general a single  $H_\infty$  controller can perform well near its corresponding equilibrium point. However, the difference between linear and nonlinear model will increase as the power command signal increases. This verifies the importance of implementing a gain-scheduled controller to deal with the nonlinearity of the wind turbine.

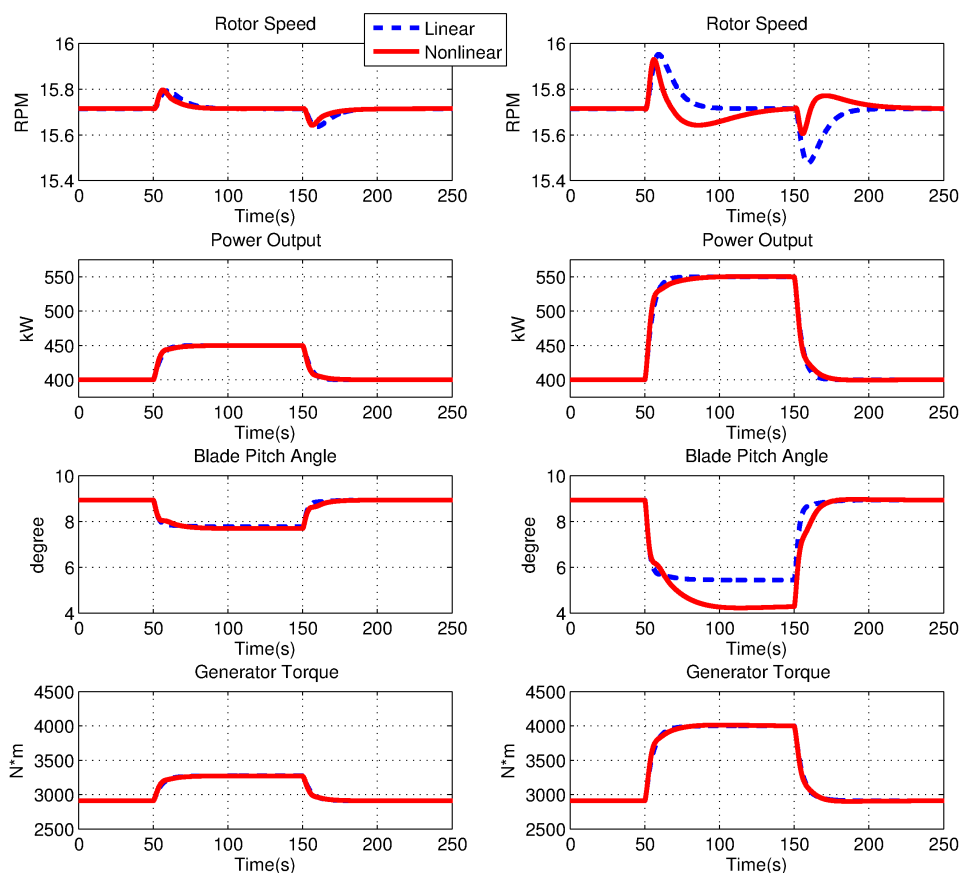


Figure 8. Simulations for a single  $H_\infty$  controller.

## B. Simulation for Gain Scheduled Controller

The second group of simulations were performed with the gain-scheduled controller designed in Section III.C. The gain-scheduled controller was simulated using the nonlinear FAST model in turbulent wind conditions.

In the first simulation, the wind profile contains 5% turbulence at a mean wind speed of 8 m/s. This corresponds to a typical Region 2 wind profile. The results are shown in Figure 9 for the gain-scheduled controller (solid line). For comparison, the figure also shows the turbine response for the the standard  $K\omega^2$  torque feedback which attempts to maximize power capture (dashed line). The subplots are, from top to bottom, the rotor speed, power capture, blade pitch, and generator torque. The power capture command for the gain-scheduled controller (dash-dot line in second subplot) steps from 400 kW to 500 kW at  $t = 150$  s,

then drops to  $300\text{ kW}$  at  $t = 300\text{ s}$  and finally steps back to  $400\text{ kW}$  at  $t = 450\text{ s}$ . The gain-scheduled controller has a 90% settling time response to the step commands of less than 10 s. In addition, the power tracking resists the fluctuations introduced by wind turbulence. Since the wind speed remains within the region 2, the rotor speed command specified in Equation 2 is proportional to the low-pass filtered wind speed estimate. This rotor speed command is shown as the dash-dot line in the top subplot. The rotor speed regulation for the gain-scheduled controller has smaller fluctuations than those observed for the standard torque feedback. To evaluate these fluctuations, define the root mean square (RMS) of the rotor speed tracking error  $\omega_{RMS}$  as:

$$\omega_{RMS} = \left( \frac{1}{T} \int_0^T |\omega - \omega_{cmd}|^2 dt \right)^{\frac{1}{2}} \quad (18)$$

$T$  is the simulation time.  $\omega$  and  $\omega_{cmd}$  are the rotor speed and its reference. Since both standard control law and APC try to track the optimal TSR  $\lambda_*$  in low wind speed, their tracking errors as defined above can be calculated. Similarly, the RMS of the pitch rate can be defined to indicate the pitch actuation. The damage equivalent loads (DEL) are also calculated to evaluate the performance of the gain-scheduled controller. All these results are shown in the first part of Table 2 which is labeled by ‘under Rated Wind’. Compared to the standard control law, there is a significant decrease in the RMS of the rotor speed tracking error for the gain-scheduled controller. At the same time, the DEL of the blade root flapwise bending moment and the tower fore-aft bending moment decrease over 20% (the exact ratio is shown in the parentheses after the value for each item). The DEL of the low speed shaft torque for the gain-scheduled controller is very close to the value for the standard control law. However, the simulation for APC in Figure 9 contains several step power command signals that lead to abrupt changes in generator torque. In order to certify the effect of these changes to the DEL, a supplementary simulation using the gain-scheduled controller is done with constant power command signal at  $500\text{ kW}$ . The results are shown in the last column of Table 2. The DEL of the low speed shaft torque decreases about 30%. These results indicate that large loads occur on the shaft during step changes in power command. These loads would be alleviated in practice by using smooth (rather than step) power command transitions. The gain-scheduled controller uses (third subplot of Figure 9) blade pitch actuation in these region 2 conditions to obtain the improved performance mentioned above. It is also shown in the rows of the ‘RMS Pitch Rate’ and the ‘Max Pitch Rate’ of Table 2. This additional pitch actuation is the extra price the gain-scheduled controller paid for APC at under rated wind speed. Finally, the maximum available power is  $581\text{ kW}$  for a steady  $8\text{ m/s}$  wind speed and the power command remains within this limit. However, there were two periods during  $t = 200\text{ s}$  to  $t = 300\text{ s}$  where the wind speed dropped sufficiently that the available power was lower than the command power. The time intervals were short enough that the impact on power tracking was negligible. The transient performance in turbulent wind conditions needs further consideration.

**Table 2. Controller Performance Comparison for Simulations in FAST**

Description	Standard Control	Gain-Scheduled	G-S Supplementary
(under Rated Wind)			
Blade Root Flapwise DEL	308.1	242.4 (−21.33%)	252.4 (−18.07%)
Tower Fore-aft DEL	4602	3550 (−22.86%)	3525 (−23.4%)
Low Speed Shaft DEL	56.45	55.87 (−1.03%)	39.69 (−29.69%)
RMS Rotor Speed Error(RPM)	0.1951	0.1027 (−47.36%)	0.1026 (−47.41%)
RMS Pitch Rate ( <i>rad/s</i> )	0	0.0022 ( <i>N/A</i> )	0.0023 ( <i>N/A</i> )
Max Pitch Rate ( <i>rad/s</i> )	0	0.0132 ( <i>N/A</i> )	0.0082 ( <i>N/A</i> )
(above Rated Wind)			
Blade Root Flapwise DEL	433.4	351.5 (−18.9%)	302.3 (−30.26%)
Tower Fore-aft DEL	7027	5919 (−15.77%)	5088 (−27.59%)
Low Speed Shaft DEL	49.6	146.7 (+195.8%)	56.41 (+13.73%)
RMS Rotor Speed Error(RPM)	0.4064	0.3707 (−8.78%)	0.4003 (−1.5%)
RMS Pitch Rate ( <i>rad/s</i> )	0.0061	0.0025 (−59.02%)	0.0025 (−59.02%)
Max Pitch Rate ( <i>rad/s</i> )	0.0201	0.0191 (−4.98%)	0.0074 (−63.18%)

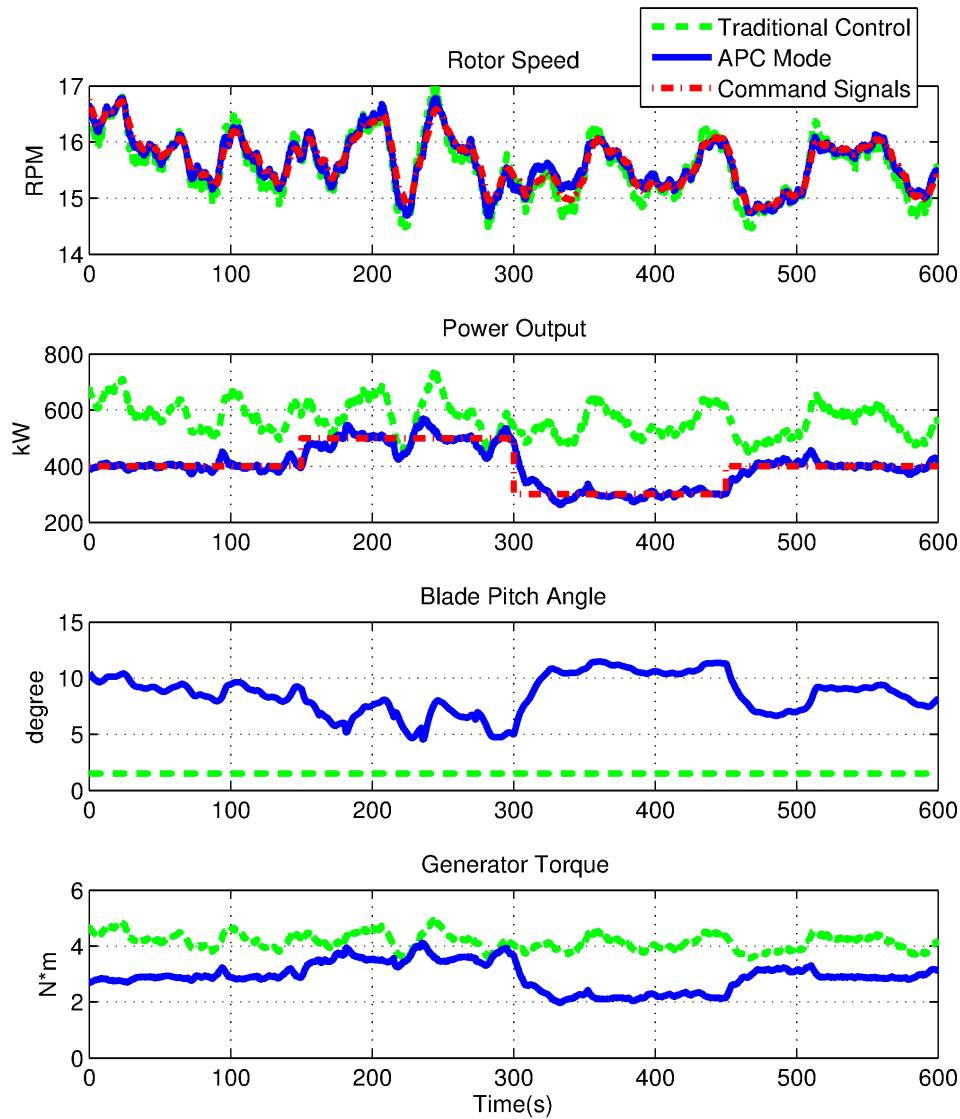


Figure 9. Simulation in below rated turbulent wind.

The second simulation was performed at an average wind speed of  $13 \text{ m/s}$  with 5% turbulence. The mean wind speed corresponds to above-rated, i.e. Region 3, wind conditions. The results are shown in Figure 10 for the gain-scheduled controller (solid line) and a traditional PI blade pitch control law (dashed line). The subplots again are, from top to bottom, the rotor speed, power capture, blade pitch, and generator torque. The power capture command for the gain-scheduled controller (dash-dot line in second subplot) steps from  $500 \text{ kW}$  to  $900 \text{ kW}$  at  $t = 150 \text{ s}$ , then drops to  $100 \text{ kW}$  at  $t = 300 \text{ s}$  and finally steps back to  $500 \text{ kW}$  at  $t = 450 \text{ s}$ . The rotor speed command for the gain-scheduled controller (Equation 2) is held fixed at the rated rotor speed (shown as dashed dot line in top subplot). Compared to the traditional PI blade pitch controller, the gain-scheduled design shows better rotor speed regulation except for the transients after step changes in power command. Since both the traditional PI controller and the gain scheduled controller try to track the rated rotor speed in high wind speed, the RMS of the tracking errors can be calculated as defined in Equation 19. The second part of Table 2 which is labeled by ‘above Rated Wind’ verifies this observation. The power tracking and disturbance rejection performance of the gain-scheduled design was also reasonable. The blade pitch actuation was smoother for the gain-scheduled design than the traditional PI controller. This is also shown in Table 2. However, the high frequency blade pitch actuation obtained with the traditional PI controller could be removed with further tuning. Finally, the generator torque for the gain-scheduled

design required additional activity to track the power commands and that leads to a significant increase (about 200%) of the low speed shaft DEL when step signal adds in. Again, a supplementary simulation using the gain-scheduled controller is done with constant power command at 900 kW. The low speed shaft DEL is about 14% over the value for the standard control law in this situation. These results again indicate that discontinuous step changes in the power command lead to a significant increase in shaft DELs. Hence smooth power commands would be required in practice to avoid large shaft loads. Finally, the DEL of the blades and the tower are much lower for the gain-scheduled controller than the standard law, especially when the power command is constant.

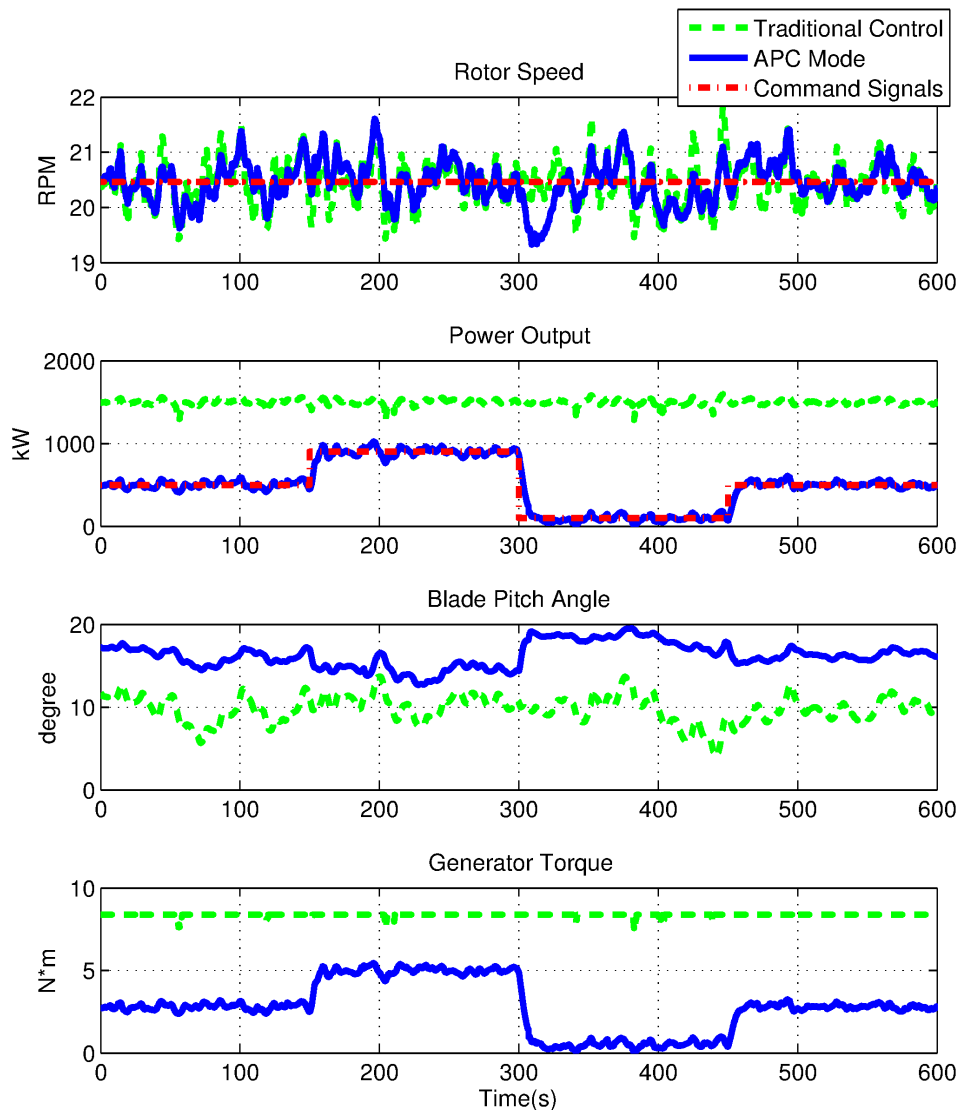


Figure 10. Simulation in above rated turbulent wind.

## V. Conclusion

This paper proposes a gain-scheduled  $H_\infty$  control design for active power control. The blade pitch and generator torque are coordinated in order to track a power command and a specific tip speed ratio. Controllers are synthesized on a grid of trim operating conditions and the gain scheduling is used to interpolate for operating between these trim points. The proposed structure enables a uniform design and operation anywhere within the power envelope of the turbine. Simulation results were provided for the feasibility assessments of this control architecture. The power tracking performance is reasonable. Simulations studies

indicate that the proposed control design shows better rotor speed tracking and lower tower/blade damage equivalent loads as compared to the standard control law. Shaft damage equivalent loads are higher for the proposed control design but still remain within acceptable limits. However, several aspects of the gain-scheduled control design need further consideration. These include the maximum power tracking bandwidth, additional outer loop controls for different ancillary services, upper bounds on the command power in turbulent wind conditions, actuator saturation, and more rigorous LPV designs.

## Acknowledgments

This work was supported by the National Science Foundation under Grant No. NSF-CMMI-1254129 entitled "CAREER: Probabilistic Tools for High Reliability Monitoring and Control of Wind Farms." The work was also supported by IREE Project RL001113, Innovating for Sustainable Electricity Systems: Integrating Variable Renewable, Regional Grids, and Distributed Resources. Any opinions, findings, and conclusions or recommendations expressed in this material are those of the authors and do not necessarily reflect the views of the National Science Foundation.

## References

- <sup>1</sup>"World Wind Energy Report 2011," *Proceedings of the 11 th World Energy Conference*, World Wind Energy Association, Bonn, Germany, 2012.
- <sup>2</sup>Crabtree, G., Misewich, J., Ambrosio, R., Clay, K., DeMartini, P., James, R., Lauby, M., Mohta, V., Moura, J., Sauer, P., et al., "Integrating Renewable Electricity on the Grid," *AIP Conference Proceedings-American Institute of Physics*, Vol. 1401, 2011, p. 387.
- <sup>3</sup>Aho, J., Bucksan, A., Laks, J., Fleming, P., Jeong, Y., Dunne, F., Churchfield, M., Pao, L., and Johnson, K., "A Tutorial of Wind Turbine Control for Supporting Grid Frequency through Active Power Control," *Proceedings of American Control Conference*, IEEE, 2012, pp. 3120–3131.
- <sup>4</sup>Rebours, Y., Kirschen, D., Trotignon, M., and Rossignol, S., "A Survey of Frequency and Voltage Control Ancillary Services-Part I: Technical Features," *IEEE Transactions on Power Systems*, Vol. 22, No. 1, 2007, pp. 350–357.
- <sup>5</sup>Burton, T., Sharpe, D., Jenkins, N., and Bossanyi, E., *Wind Energy Handbook*, John Wiley & Sons, 1st ed., 2001.
- <sup>6</sup>Greedy, L., "Review of electrical drive-train topologies," *Project UpWind, Mekelweg, the Netherlands and Aalborg East, Denmark, Tech. Rep.*, 2007.
- <sup>7</sup>Nelson, R. J., "Frequency-Responsive Wind Turbine Output Control," 2011, U.S. Patent 0 001 318.
- <sup>8</sup>Keung, P.-K., Li, P., Banakar, H., and Ooi, B. T., "Kinetic Energy of Wind Turbine Generators for System Frequency Support," *IEEE Transactions on Power Systems*, Vol. 24, No. 1, 2009, pp. 279–287.
- <sup>9</sup>Juankorena, X., Esandi, I., López, J., and Marroyo, L., "Method to Enable Variable Speed Wind Turbine Primary Regulation," *International Conference on Power Engineering, Energy and Electrical Drives, 2009*, IEEE, 2009, pp. 495–500.
- <sup>10</sup>Aho, J., Bucksan, A., Pao, L., and Fleming, P., "An Active Power Control System for Wind Turbines Capable of Primary and Secondary Frequency Control for Supporting Grid Reliability," *51st AIAA Aerospace Sciences Meeting including the New Horizons Forum and Aerospace Exposition*, 2013, pp. AIAA 2013–0456.
- <sup>11</sup>Acedo Sanchez, J., Carcar, M., Lusarreta, M., Perez Barbachano, J., Simon Segura, S., Sole Lopez, D., Zabaleta Maeztu, M., Marroyo Palomo, L., Lopez Taberna, J., et al., "Method of Operation of A Wind Turbine to Guarantee Primary or Secondary Regulation in An Electric Grid," 2011, U.S. Patent 0 057 445.
- <sup>12</sup>Jeong, Y., Johnson, K., and Fleming, P., "Comparison and testing of power reserve control strategies for grid-connected wind turbines," *Wind Energy*, 2013.
- <sup>13</sup>Apkarian, P., Gahinet, P., and Becker, G., "Self-scheduled  $H_\infty$  Control of Linear Parameter-varying Systems: a Design Examples," *Automatica*, Vol. 31, No. 9, 1995, pp. 1251–1261.
- <sup>14</sup>Bobanac, V., Jelavić, M., and Perić, N., "Linear Parameter Varying Approach to Wind Turbine Control," *14th International Power Electronics and Motion Control Conference*, 2010, pp. T12–60–T12–67.
- <sup>15</sup>Manwell, J., McGowan, J., and Rogers, A., *Wind Energy Explained: Theory, Design, and Application*, Wiley, 2010.
- <sup>16</sup>Jonkman, J. and Buhl, M., *FAST User's Guide*, National Renewable Energy Laboratory, Golden, Colorado, 2005.
- <sup>17</sup>Bossanyi, E., "The design of closed loop controllers for wind turbines," *Wind Energy*, Vol. 3, 2000, pp. 149–163.
- <sup>18</sup>Laks, J., Pao, L., and Wright, A., "Control of Wind Turbines: Past, Present, and Future," *Proceedings of American Control Conference*, 2009, pp. 2096–2103.
- <sup>19</sup>Johnson, K., Pao, L., Balas, M., and Fingersh, L., "Control of variable-speed wind turbines: standard and adaptive techniques for maximizing energy capture," *IEEE Control System Magazine*, Vol. 26, No. 3, 2006, pp. 70–81.
- <sup>20</sup>Bossanyi, E. A., "Individual Blade Pitch Control for Load Reduction," *Wind Energy*, Vol. 6, No. 2, 2003, pp. 119–128.
- <sup>21</sup>Stol, K., Zhao, W., and Wright, A., "Individual blade pitch control for the controls advanced research turbine (CART)," *Journal of Solar Energy Engineering*, Vol. 128, 2006, pp. 498.
- <sup>22</sup>Laks, J., Pao, L., Wright, A., Kelley, N., and Jonkman, B., "Blade pitch control with preview wind measurements," *48th AIAA Aerospace Sciences Meeting and Exhibit*, 2010, pp. AIAA–2010–251.
- <sup>23</sup>Laks, J., Pao, L., and Wright, A., "Combined Feed-forward/Feedback Control of Wind Turbines to Reduce Blade Flap Bending Moments," *47th AIAA Aerospace Sciences Meeting*, 2009, pp. AIAA–2009–687.

- <sup>24</sup>Stol, K. and Balas, M., “Full-State Feedback Control of a Variable-Speed Wind Turbine: A Comparison of Periodic and Constant Gains,” *Journal of Solar Energy Engineering*, Vol. 123, No. 4, 2001, pp. 319–326.
- <sup>25</sup>Stol, K. and Balas, M., “Periodic Disturbance Accommodating Control for Blade Load Mitigation in Wind Turbines,” *Journal of Solar Energy Engineering*, Vol. 125, No. 4, 2003, pp. 379–385.
- <sup>26</sup>Wright, A. and Balas, M., “Design of Controls to Attenuate Loads in the Controls Advanced Research Turbine,” *Journal of Solar Energy Engineering*, Vol. 126, No. 4, 2004, pp. 1083–1091.
- <sup>27</sup>Tarnowski, G., Kjær, P., Dalsgaard, S., and Nyborg, A., “Regulation and Frequency Response Service Capability of Modern Wind Power Plants,” *Proceedings of IEEE Power and Energy Society General Meeting*, 2010, pp. 1–8.
- <sup>28</sup>Packard, A., “Gain Scheduling via Linear Fractional Transformations,” *Systems and Control Letters*, Vol. 22, 1994, pp. 79–92.
- <sup>29</sup>Apkarian, P. and Gahinet, P., “A Convex Characterization of Gain-scheduled  $H_\infty$  Controllers,” *IEEE Transactions on Automatic Control*, Vol. 40, No. 5, 1995, pp. 853–864.
- <sup>30</sup>Mikkelsen, T., Hansen, K., Angelou, N., Sjöholm, M., Harris, M., Hadley, P., Scullion, R., Ellis, G., and Vives, G., “Lidar wind speed measurements from a rotating spinner,” *Proc. European Wind Energy Conference, Warsaw, Poland*, 2010.
- <sup>31</sup>Knudsen, T., Bak, T., and Soltani, M., “Prediction models for wind speed at turbine locations in a wind farm,” *Wind Energy*, Vol. 14, No. 7, 2011, pp. 877–894.
- <sup>32</sup>Zhou, K., Doyle, J. C., and Glover, K., *Robust and Optimal Control, 1st Edition*, Prentice Hall, 1996.
- <sup>33</sup>Skogestad, S. and Postlethwaite, I., *Multivariable Feedback Control*, John Wiley and Sons Ltd., 2007.